# TRANSFORMER EQUIVALENT NETWORK FOR SWITCHING SURGE STUDIES

by

Dr. J.R. Lucas

ARTICLE NO. 4

## Abstract

For the calculation of switching surges on transformer feeders, it is desirable that all the system components be adequately represented mathematically. In this paper a representation of the transformer is described which is suitable for use in these calculations. The representation is based on the transformer being viewed as a set of primitive windings with winding interconnections being performed with connection matrices. This method, not only accurately models the transformer under varying frequency conditions but also permits a single representation to be used for all common winding configurations. Single pole energisation of a 84 mile long transformer feeder is considered and results obtained from the computer study are compared with field results. The analysis shows that improper representation of the transformer results in grossly inadmissible results.

## List of Principal Symbols

| | |
|---|---|
| [A], [B] | Two port admittance matrix parameters of line |
| $[C_{eq}]$ | Equivalent winding capacitance matrix |
| [CON] | Connection matrix indicating winding type |
| $[G_{eq}]$ | Equivalent winding conductance matrix |
| $\underline{i}$ | Internal winding current vector |
| $\underline{I}$ | Transformer phase current vector |
| $\underline{I}_L$ | Line current vector at transformer terminal |
| $\underline{I}_s, \underline{I}_r, \underline{I}_t$ | Line current vectors at positions s, r, t |
| [L] | Transformer inductance matrix |
| p | Fourier transform operator |
| $[R_o]$ | Core loss resistance matrix |
| $[S_{eq}]$ | Equivalent inverse inductance matrix |
| [U] | Connection matrix |
| $\underline{V}$ | Transformer voltage vector |
| $\underline{V}_s, \underline{V}_r, \underline{V}_t$ | Voltage vectors at positions s, r, t |
| $[Y_p]$ | Combined Transformer / Load admittance matrix |
| $[Y_t]$ | Terminal Load admittance matrix |
| $[Y_{tf}]$ | Transformer admittance matrix |

Dr. J.R. Lucas, BSc(Eng), MSc, PhD, CEng, FIEE, FIE(Sri Lanka), MCS(Sri Lanka) is a Senior Lecturer in Electrical Engineering and is the Head of the Division of Power System & High Voltage Engineering at the University of Moratuwa. He graduated in Electrical Engineering from the University of Ceylon, Peradeniya in 1969 and completed his post-graduate studies at the University of Manchester Institute of Science and Technology, U.K. in 1974.

## 1. Introduction

The prediction of switching overvoltages in electrical transmission systems is of increasing economic importance. Prediction of switching overvoltages at the design stage of a system can result in measures being taken to reduce the overvoltages, resulting in reduced insulation requirements. Prediction of switching overvoltages in a system already operating can indicate how changes in system operation might obviate the overvoltages, resulting in lower outage rates.

When switching overvoltage calculations are to be made by the digital computer, it is first necessary to convert the complex electromagnetic and electrostatic fields of each component of the system into an equivalent network. It is then necessary to assemble the individual networks into an overall equivalent network that represents the entire transmission system. Finally, mathematical techniques have to be developed in order that solutions may be obtained to the resulting network equations.

In the past, the equivalent network for the transmission line has been extensively developed and a number of techniques are available for obtaining solutions to the network equations[1-4]. On the other hand, the equivalent networks of transformers for use in switching surge studies have received little attention. Consequently, the calculation of switching overvoltages in transmission systems has generally been undertaken with a very accurate representation of the transmission line, but only a superficial representation of the system transformers.

For power frequency studies, the equivalent network of the multiwinding transformer is governed almost entirely by electromagnetic considerations. For surge distribution studies, the equivalent network of the transformer has to represent the complex high frequency electromagnetic and electrostatic fields of the winding. Consequently, a highly detailed representation of the winding is necessary, and the equivalent network usually takes the form of an extensive distributed parameter network[5].

In representing the transformer in switching surge calculations, it is necessary to consider the range of natural frequencies of power transformers and the component frequencies encountered in switching surge waveforms. Harner and Rodriguez[6] in an extensive study on the characteristics of transformers under fault conditions reported natural frequencies in the range 0.5 to 50 kHz. Binns and Habibollahi[7] in a frequency analysis study of switching surge waveshapes observed that the major frequency components were within the range 100 Hz to 1 kHz for the system studied. The equivalent network of the transformer for switching surge studies must therefore be valid over the range of frequencies from 50 Hz to 50 kHz. As a consequence of this, an equivalent network of the type used for surge distribution purposes will be too elaborate and an equivalent network of the type used for power frequency studies will be insufficient.

The purpose of the present paper will, therefore be to develop an equivalent network of the transformer for use in switching surge calculations. In the equivalent network, the distributed capacitance and inductance of the windings will be represented by lumped elements. Although this simplification will neglect the travelling wave properties of the windings, inaccuracies result only in the case of extremely high speed wavefronts rarely encountered in switching surge studies. Since three phase transformers are considered in the present studies, the mutual magnetic coupling between windings is taken into account. Furthermore, provision is made for formulating all inductances as frequency dependant parameters, for it has been shown that the inductance of transformer windings is frequency dependant[8,9] over the range of frequencies considered. Primary to secondary, interturn and winding to earth capacitances are represented by lumped equivalents. Capacitance between windings of different phases can also be represented, if these are not negligibly small.

Considering the multiplicity of components and the need within the representation to allow for a number of terminal connections, it is desirable to have a representation within which the winding connections can easily be rearranged. For this purpose, the equivalent network is formed as a primitive set of windings which are interconnected as required by a connection matrix.

In recent years, Fourier transform techniques[10] have been applied to switching surge problems in transmission systems and have been shown to be extremely powerful. In the technique, frequency dependant parameters can be included without difficulty. Consequently, the present work[11] is based on taking due account of frequency dependant parameters by the use of the Fourier transform technique in the solution of the network equations. The emphasise of the present paper will be on the development of the equivalent network rather than on a detailed study of the parameters involved.

## 2. Single Phase Transformer

A single phase, two-winding transformer can be represented by two magnetically coupled windings, together with lumped capacitance elements, as shown in Fig. 1. For most transformer connections, terminals 1' and 2' will be connected to earth, so that the capacitance elements $C_{e1}$, $C_{e2}$ and $C_{21}$ will not enter into the calculations. These elements have, however, been included, in order that the representation can be perfectly general and cover such cases as transformers with delta windings or unearthed star windings and series reactors.

With all voltages being specified with respect to earth, equating the currents at each node, the following equation is obtained.

$$\begin{bmatrix} I_1 \\ I_2 \\ -I_1' \\ -I_2' \end{bmatrix} = \begin{bmatrix} 1 & 0 \\ 0 & 1 \\ -1 & 0 \\ 0 & -1 \end{bmatrix} \begin{bmatrix} i_1 \\ i_2 \end{bmatrix} + p \begin{bmatrix} C_{1e}+C_{11}+C_{12} & -C_{12} & -C_{11} & 0 \\ -C_{12} & C_{2e}+C_{22}+C_{12} & 0 & -C_{22} \\ -C_{11} & 0 & C_{e1}+C_{11}+C_{21} & -C_{21} \\ 0 & -C_{22} & -C_{22} & C_{2}+C_{22}+C_{21} \end{bmatrix} \begin{bmatrix} V_1 \\ V_2 \\ V_1' \\ V_2' \end{bmatrix}$$

In compact notation,

$$\underline{I} = [U]\,\underline{i} + p\,[C_{eq}]\,\underline{V} \qquad (1)$$

The voltages across the windings may be expressed as

$$\begin{bmatrix} 1 & 0 & -1 & 0 \\ 0 & 1 & 0 & -1 \end{bmatrix} \begin{bmatrix} V_1 \\ V_2 \\ V_1' \\ V_2' \end{bmatrix} = p \begin{bmatrix} L_1 & M_{12} \\ M_{21} & L_2 \end{bmatrix} \begin{bmatrix} i_1 \\ i_2 \end{bmatrix}$$

In compact notation,

$$[U]^t\,\underline{V} = p[L]\,\underline{i} \qquad (2)$$

Since $\underline{i}$ is the vector of internal currents, it is eliminated, resulting in the general equation of terminal voltages and currents given by

$$\underline{I} = \frac{1}{p}\,[U]\,[L]^{-1}\,[U]_t\underline{V} + p[C_{eq}]\underline{V} \qquad (3)$$

In compact notation,

$$\underline{I} = \frac{1}{p}\,[S_{eq}] + p[C_{eq}]\;\underline{V} \qquad (4)$$

where $[S_{eq}] = \frac{1}{p}\,[U]\,[L]^{-1}\,[U]^t$

For the case where both windings are solidly earthed at one end, voltage $V_1'$ and $V_2'$ are zero, and only the non-earthed terminal currents are of interest. In this case, equation (4) will have the vectors $\underline{I}$ and $\underline{V}$ reduced to two terms, and the matrices $[S_{eq}]$ and $[C_{eq}]$ will be of order 2x2.

## 3. General Three Phase Transformer

### 3.1 Primitive windings

The derivations for the general single phase case can readily be extended to the general three phase case. However, in this case, it is more convenient to separate the voltage vector into two vectors corresponding to the two ends of the winding, and to reexpress equation (2) in the form

$$\underline{V} - \underline{V}' = p\,[L]\,\underline{i} \qquad (5)$$

where L contains the mutual coupling between the phases as well. It is also sufficient to express the currents at only one end of each winding in equation (1), which may then be rewritten in the form

$$\underline{I} = \underline{i} + p[C_e]\,\underline{V} - p[C_e']\,\underline{V}'$$

or in the more convenient form

$$\underline{I} = \underline{i} + p\,[C_e] - [C_e']\quad \underline{V} \;+$$

$$p[C_e']\,(\underline{V} - \underline{V}') \qquad (6)$$

where $[C_e]$ and $[C_e']$ include all relevant lumped capacitances.

### 3.2 Connection Matrices for delta and star connections

In the delta winding, the start of one phase-winding is connected to the end of another phase-winding. This is shown in fig. 2a, and for this we can write

$$\begin{bmatrix} V_1' \\ V_2' \\ V_3' \end{bmatrix} = \begin{bmatrix} 0 & 1 & 0 \\ 0 & 0 & 1 \\ 1 & 0 & 0 \end{bmatrix} \begin{bmatrix} V_1 \\ V_2 \\ V_3 \end{bmatrix} \qquad (7)$$

and the difference voltages may be written

$$\begin{bmatrix} V_1 - V_1' \\ V_2 - V_2' \\ V_3 - V_3' \end{bmatrix} = \begin{bmatrix} 1 & -1 & 0 \\ 0 & 1 & -1 \\ -1 & 0 & 1 \end{bmatrix} \begin{bmatrix} V_1 \\ V_2 \\ V_3 \end{bmatrix}$$

or in compact notation

$$\underline{V} - \underline{V}' = [CON_D]\,\underline{V} \qquad (8)$$

Similarly, if an earthed star winding is considered, fig. 2b, then

$$V_1' = V_2' = V_3' = 0$$

so that

$$\begin{bmatrix} V_1 - V_1' \\ V_2 - V_2' \\ V_3 - V_3' \end{bmatrix} = \begin{bmatrix} 1 & 0 & 0 \\ 0 & 1 & 0 \\ 0 & 0 & 1 \end{bmatrix} \begin{bmatrix} V_1 \\ V_2 \\ V_3 \end{bmatrix}$$

or in compact notation

$$\underline{V} - \underline{V}' = [CON_S]\,\underline{V} \qquad (9)$$

By compounding the connection matrices in equations (8) and (9), the total connection matrix [CON] for a multi-winding transformer may be formed.

Thus, for a multi-winding transformer we may write

$$\underline{V} - \underline{V}' = [CON]\underline{V} \qquad (10)$$

Substituting equation (10) into equation (5) gives

$$[CON]\,\underline{V} = p[L]\,\underline{i}$$

or, the internal currents may be expressed as

$$\underline{i} = \frac{1}{p}\,[L]^{-1}\,[CON]\,\underline{V} \qquad (11)$$

Substituting the result of equation (10) in equation (6) gives

$$\underline{I} = \underline{i} + p\left[[C_e] - [C_e']\right]\underline{V} + p[C_e']\,[CON]\,\underline{V} \qquad (12)$$

Substitution of equation (11) in equation (12) results in

$$\underline{I} = \frac{1}{p}\,[L]^{-1}\,[CON]\,\underline{V} + p\left[[C_e] - C_e'\right]\underline{V} + p\,[C_e']\,[CON]\,\underline{V} \qquad (13)$$

It is, however, the line currents $\underline{I}_L$ and not the currents I that are usually required and for this purpose, it can be easily shown that

$$\underline{I}_L = [CON]^t\,\underline{I} \qquad (14)$$

The line currents of the transformer can now be found from

$$\underline{I}_L = \frac{1}{p}\,[CON]^t[L]^{-1}[CON]\underline{V} + p[CON]^t\left[[C_e] - [C_e'] + [C_e']\,[CON]\right]\underline{V} \qquad (15)$$

In compact notation this may be written

$$\underline{I}_L = \left[\frac{1}{p}\,[S_{eq}] + p[C_{eq}]\right]\underline{V} \qquad (16)$$

where

$$[S_{eq}] = [CON]^t[L]^{-1}[CON]$$

and

$$[C_{eq}] = [CON]^t\left[[C_e] - C_e' + [C_e']\,[CON]\right]\underline{V}$$

Equation (16) may also be written in the form

$$\underline{I}_L = [Y_{tf}]\,\underline{V} \qquad (16a)$$

where

$[Y_{tf}]$ = transformer equivalent admittance matrix

Equation (16) thus relates all the terminal currents with the voltages to earth at the terminals of the transformer. The matrices $[S_{eq}]$ and $[C_{eq}]$ do not contain any frequency terms and therefore need to be calculated only once for use in the modified Fourier analysis. However, the variation of inductance with frequency will have to be accounted for by a multiplication of $[S_{eq}]$ by a suitable factor at each frequency step in the analysis.

A similar analysis can be carried out for the unearthed star connection. However, the final equation then obtained cannot be simplified in the same manner and the solution requires matrix inversion at each frequency step.

## 4. Transformers with Tertiary Windings

The theory for the three-winding transformer can quite easily be obtained by extending the theory already derived for the two-winding transformer. However, in the case of three winding transformers, $\underline{I}_L$ and $\underline{V}$ are both vectors containing nine elements, and the matrices involved are of the order 9x9.

If the tertiary winding is terminated in a load such as a capacitor or reactor bank, then the tertiary voltages and currents may be eliminated and an equivalent two port admittance matrix may be obtained. This takes into full account the effect of the tertiary connection and its loading, although the tertiary voltages and currents are not directly available.

## 5. Autotransformers

In the case of the auto-transformer, the foregoing analysis can be applied provided some minor alterations are made in the basic winding equations.

## 6. Inclusion of Losses

At normal supply frequencies, the modern power transformer has a high efficiency, and copper and iron losses are very small. However, in transient analysis, frequencies much higher than power frequencies are present and iron losses are known to be frequency dependant. Consequently, although very little information is available on the variation of transformer losses with frequency, it is considered desirable, for completeness, to make provision for the inclusion of losses within the formulation.

Core losses may be conveniently represented by suitable shunt resistances across the winding, frequency dependent as required. This requires some additional formulation procedures which are indicated in the following sections.

### 6.1 Delta connected windings

In the delta connected winding shown in fig. 3a, the resistive elements represent the frequency dependent iron loss components of the windings. The currents circulating in these loss paths may be written

$$\begin{bmatrix} I_1' - I_1 \\ I_2' - I_2 \\ I_3' - I_3 \end{bmatrix} = \begin{bmatrix} 1/R_1 & 0 & 0 \\ 0 & 1/R_2 & 0 \\ 0 & 0 & 1/R_3 \end{bmatrix} \begin{bmatrix} V_1 - V_2 \\ V_2 - V_3 \\ V_3 - V_1 \end{bmatrix}$$

or in compact notation

$$\underline{I}' - I = \left[R_p^{-1}\right] \underline{V}_D \qquad (17)$$

These resistor currents may be related to the line currents by the delta-connection matrix $[CON_D]^t$ used earlier, so that

$$\underline{I}_L' - \underline{I}_L = [CON_D]^t \; (\underline{I}' - I) \qquad (18)$$

Furthermore, the difference voltages of equation (17) may be related to the line voltages by the delta-connection matrix $[CON_D]$, so that

$$\underline{V}_D = [CON_D] \; \underline{V} \qquad (19)$$

Substitution in equation (18) gives

$$\underline{I}'_L - I_L = [CON_D]^t \, [R_p^{-1}] \, [CON_D] \, \underline{V} \qquad (20)$$

Thus the equivalent conductance matrix of the delta connected winding is

$$[G_{eq}] = [CON_D]^t \, [R_p^{-1}] \, [CON_D]$$

**6.2 Star connected windings**

By a similar-derivation to that of the delta winding, and with reference to fig. 3b, the resistive current for the star winding is found to be

$$\begin{bmatrix} I'_1 - I_1 \\ I'_2 - I_2 \\ I'_3 - I_3 \end{bmatrix} = \begin{bmatrix} 1/R_1 & 0 & 0 \\ 0 & 1/R_2 & 0 \\ 0 & 0 & 1/R_3 \end{bmatrix} \begin{bmatrix} V_1 \\ V_2 \\ V_3 \end{bmatrix}$$

or in compact notation

$$\underline{I}' - \underline{I} = [R_p^{-1}] \, \underline{V}$$

For the star winding, the phase currents are equal to the line currents so that

$$\underline{I}'_L - \underline{I}_L = [R_p^{-1}] \, \underline{V} \qquad (21)$$

and the equivalent conductance matrix of the star connected winding is

$$[G_{eq}] = [R_p^{-1}]$$

When multi-winding transformers are considered, the total equivalent conductance matrix is composed of the sub-matrices $[G_{eq}]$. The total equivalent conductance matrix is added to the transformer admittance matrix. The resultant admittance matrix is the complete admittance matrix to be used in the analysis.

Since Fourier analysis is used in the calculations, the admittance matrix can be computed at each frequency step and any dependence of the core loss with frequency can be easily accommodated by claculating the equivalent conductance values at each frequency.

## 7. Energisation of a Transformer from a Transmission Line

One frequency encountered overvoltage problem in transmission systems is the generation of overvoltages at a transformer supplied from a long transmission line. Fig. 4 shows the equivalent circuit for a loaded transformer fed from a transmission line.

The currents and voltages at the terminal load are related by

$$\underline{I}_t = [Y_t] \, \underline{V}_t \qquad (22)$$

For the convenience of analysis, the transformer admittance matrix is partitioned into primary/secondary sub-matrices, and equation (16a) may be written as

$$\begin{bmatrix} \underline{I}_r \\ -\underline{I}_t \end{bmatrix} = \begin{bmatrix} [Y_{tf11}] & [Y_{tf12}] \\ [Y_{tf21}] & [Y_{tf22}] \end{bmatrix} \begin{bmatrix} \underline{V}_r \\ \underline{V}_t \end{bmatrix} \qquad (23)$$

Combining equations (22) and (23) gives

$$\begin{bmatrix} \underline{I}_r \\ \underline{O} \end{bmatrix} = \begin{bmatrix} [Y_{tf11}] & [Y_{tf12}] \\ [Y_{tf21}] & [Y_{tf22}] + [Y_t] \end{bmatrix} \begin{bmatrix} \underline{V}_r \\ \underline{V}_t \end{bmatrix} \qquad (24)$$

from which $\underline{V}_t$ is eliminated to give

$$\underline{I}_r = \left[ [Y_{tf11}] - [Y_{tf12}] \left[ [Y_{tf22}] + [Y_t] \right]^{-1} [Y_{tf21}] \right] \underline{V}_r \qquad (25)$$

which in compact notation can be written as

$$\underline{I}_r = [Y_p] \, \underline{V}_r \qquad (26)$$

where

$$[Y_p] = [Y_{tf11}] - [Y_{tf12}] \Big[ [Y_{tf22}] + [Y_t] \Big]^{-1} [Y_{tf21}]$$

$|Y_p|$ represents the combined admittance matrix of the transformer and load as viewed from the transformer primary terminals.

The two port admittance matrix of the transmission line[10] may be written as

$$\begin{bmatrix} \underline{I}_s \\ -\underline{I}_r \end{bmatrix} = \begin{bmatrix} [A] & -[B] \\ [B] & [A] \end{bmatrix} \begin{bmatrix} \underline{V}_s \\ \underline{V}_r \end{bmatrix} \tag{27}$$

From equation (26), substituting for $\underline{I}_r$ in equation (27) and rearranging leads to

$$\begin{bmatrix} \underline{I}_s \\ \underline{O} \end{bmatrix} = \begin{bmatrix} A & -B \\ -B & A+Y_p \end{bmatrix} \begin{bmatrix} \underline{V}_s \\ \underline{V}_r \end{bmatrix} \tag{28}$$

In the case of single pole energisation of a circuit breaker (i.e. for the first phase to close), the applied voltage conditions for the first phase are known at the sending end of the line. Further, the sending end currents of the other two phases are also zero.

Thus equation (28) may be solved to give the unknown voltages and currents in the transform domain. By systematically working backwards, the transforms of all the unknown voltages and currents may be determined in the transform domain. The inverse Fourier transform then gives the transient solution in the time domain.

## 8. Computer Study

To demonstrate the importance of the transformer model, a study was carried out on the transformer feeder shown in fig. 5.

This particular system was selected as field test results are available for a similar system, which is used in the present paper for comparison of computer results. The field oscillograms obtained by Price et Al[12] are for the sequential closure of the circuit breaker at A, with the second pole closing approximately 6½ ms after the first pole closure. The receiving and transformer in the field test is a three-phase transformer with a $\lambda - \lambda - \blacktriangleright$ configuration.

In order to justify the importance of the transformer winding configuration on switching surges, computations were carried out for the actual configuration of - - - as well as for a - - - configuration. Further, to show the importance of considering the interlimb magnetic coupling in the transformer core, the - - configuration was considered with and without interlimb magnetic coupling. These two cases of coupling, infact correspond to a three-phase transformer, and a bank of three single-phase transformers.

In the study, only the first pole to close to of the sequential closure was considered and the comparison was made upto the instant of the closure of the second pole in the field test. Exact comparison was not possible as some of the parameters of the test system were not available and some suitable assumptions had to be made.

The transmission line considered was of a typical configuration, and the rest of the power system supplying the line was represented by its Thevenin's equivalent.

The transformer at the receiving end of the line was given the following data.

| | | |
|---|---|---|
| Rating of transformer | = | 300 MVA |
| Voltage of primary | = | 345 kV |
| Voltage of secondary | = | 138 kV |
| Voltage of tertiary | = | 33 kV |
| Magnetising current | = | 0.5% |
| Core less current | = | 1.0% |
| Primary leakage inductance | = | 5.0% |
| Secondary leakage inductance | = | 5.0% |
| Tertiary leakage inductance | = | 5.0% |

Figure 6(a) shows the three-phase voltages of the sending end of the field test oscillogram. Waveform $e_{s1}$ shows the first phase to close at the instant Ø1-C and $e_{s2}$ and $e_{s3}$ are the waveforms of the unenergised phases. It is seen that the unenergised phases have bascially the same waveform upto the energisation of the second phase at instant Ø2-C.

Figure 7(a) shows the three-phase voltages of the receiving end of the field test oscillogram. Waveform $e_{r1}$ corresponds to the energised phase, while $e_{r2}$ and $e_{r3}$ correspond to the unenergised phases.

## 9. Results

To investigate the possibility of disregarding the transformer configuration in transient calculations, the system was first analysed with a λ-λ-λ transformer at the receiving end. The computer results of Figure 6(b)(i) and figure 7(b)(i) show that both the sending end voltage waveforms and the receiving end voltage waveforms do not show any significant voltage on the unenergised phases unlike in the field test result. This is due to the absence of the delta winding on the tertiary. Studies also showed the receiving end voltages in this case is similar to that of the open circuited line.

The presence of a delta winding on either the secondary or the tertiary, such as in λ-▷-λ or λ-λ-▷ transformers, causes a significant voltage on the unenergised phase, as seen from figures 6(b)(ii) & (iii) and 7(b)(ii) & (iii). These are also seen to be similar to those in the field oscillogram. However, the period of the oscillation is not quite the same when inter-limb magnetic coupling is absent. Also, while the receiving end waveforms with inter-limb magnetic coupling (Figure 7(b)(iii)) agree in the basic shape of the receiving end waveform of the energised phase, the waveform in the absence of mutual coupling (Figure 7(b)(ii)) is completely different in the transient overvoltages.

## 10. Conclusion

The present study has used the Fast Fourier Transform with connection matrices to form the winding configuration matrices of the transformer. It has compared the transient response of an 84 mile transformer feeder obtained from field tests for a λ-λ-▷ transformer with inter-limb magnetic coupling, with analytic results for λ-λ-λ transformers and λ-λ-▷ transformers with and without inter-limb magnetic coupling. The results obtained show conclusively that only the proper configuration even gives results which are reasonably close.

## 11. Acknowledgements

The Author wishes to thank Mr. Keith Cornick, Lecturer, UMIST, Manchester for the guidance given to him during the early years

of this study. He also wishes to thank the Staff of the Department of Electrical Engineering, University of Moratuwa, and the staff of the Computer Centre, for the assistance they have always given him.

## 12. References


1. Wedepohl, L.M. and Mohamed, S.E.T., "Multiconductor transmission lines. Theory of natural modes and Fourier integrals applied to transient analysis" Proc. I.E.E., 1969, 116(9), p 1553-1563.
2. Dommel, H.W., "Digital computer solutions of electromagnetic transients in single and multiphase networks" Trans IEEE, 1969, PAS-88(4), p 388-399.
3. Thoren, H.B. and Carlsson, K.L., "A digital computer program for the calculation of switching and lightning surges on power systems", Trans IEEE, 1970, PAS-89(2), p 212-218.
4. Rau, N.S. and Janischewskyj, W., "A numerical method for the calculation of transients in linear and non-linear transmission lines - state equations approach", Trans IEEE, 1972, PAS-91(6), p 2545-2552.
5. Lewis, T.J., "The transient behaviour of ladder networks of the type representing transformer and machine windings" Proc IEE, 1954, 101(2), p541-553.
6. Harner, R.H. and Rodriguez, J. "Transient recovery voltages associated with power system, three-phase transformer secondary faults", Trans IEEE, 1972, PAS-91(5), p 1887-1895.
7. Binns, D.F. and Habibollahi, H., "Frequency content of switching over voltages", Proc. I.E.E., 1976, 123(9), p 913-915.
8. Pirenne, J.M., "General theory of oscillatory phenomena in transformer windings (in French)" Rev. G. de E., 1940, 47(1-2), p 19-29.
9. Fergestad, P.I. and Henriksen, T., "Inductances for the calculation of transient oscillations in transformers", Trans IEEE, 1974, PAS-93(2), p 510-517.
10. Wedepohl, L.M. and Mohamed, S.E.T., "Transient analysis of multiconductor transmission lines with special reference to non-linear problems", Proc. I.E.E., 1970, 117(5), p 979-988.
11. Lucas, J.R., "Representation of Transformers in Switching Surge Studies", PhD Thesis, UMIST, 1974.
12. Price, W.S., McElroy, A.J., Smith, H.M., and Shankle, D.F., "Field Measurements of 345 kV Lightning Arrestor Switching Surge Performance", AIEE Trans, Aug 1963, p 487-500.

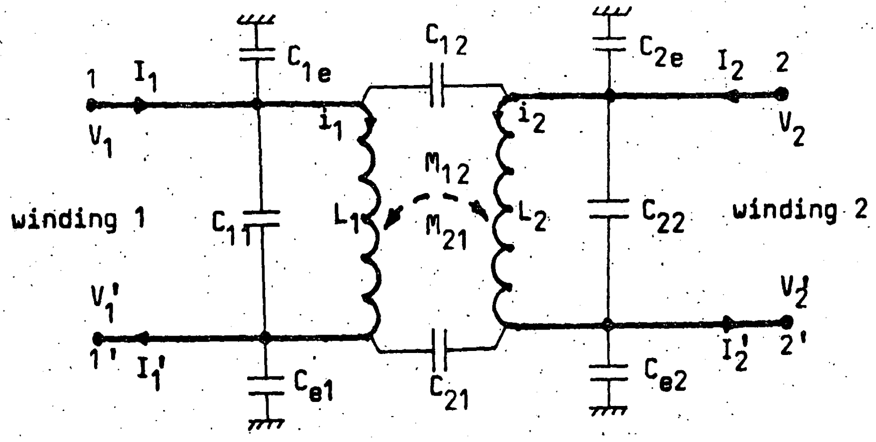


FIG 1 - SINGLE PHASE TRANSFORMER REPRESENTATION

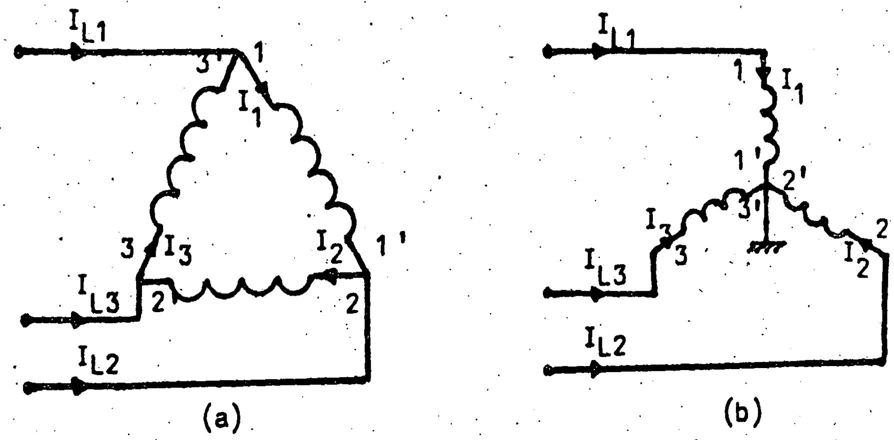


FIG 2 - DELTA AND STAR END-CONNECTIONS

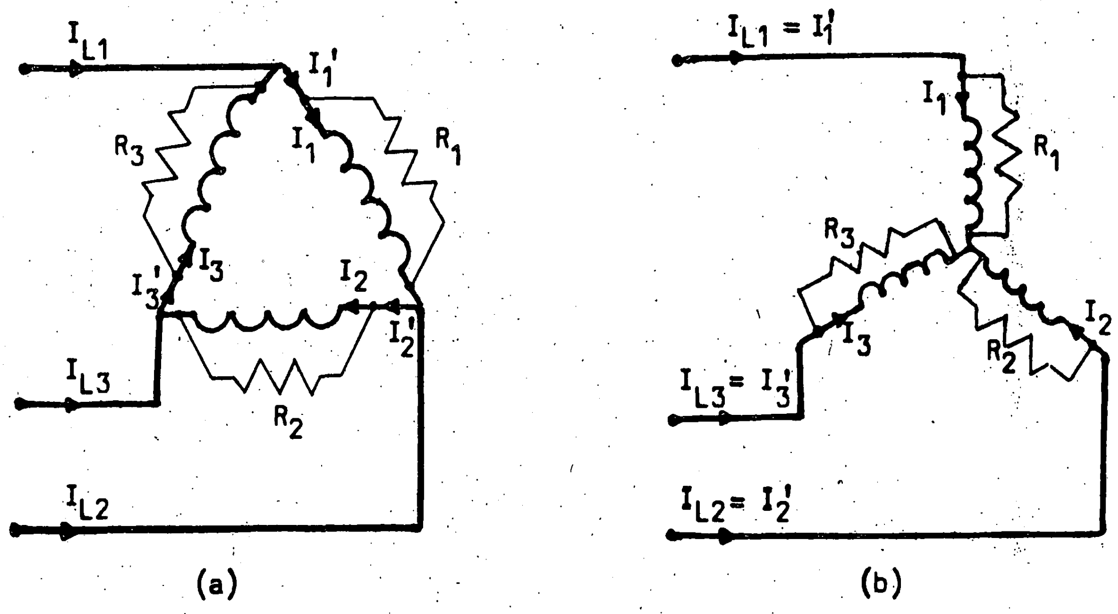


FIG 3 - INCLUSION OF LOSSES IN THE WINDING

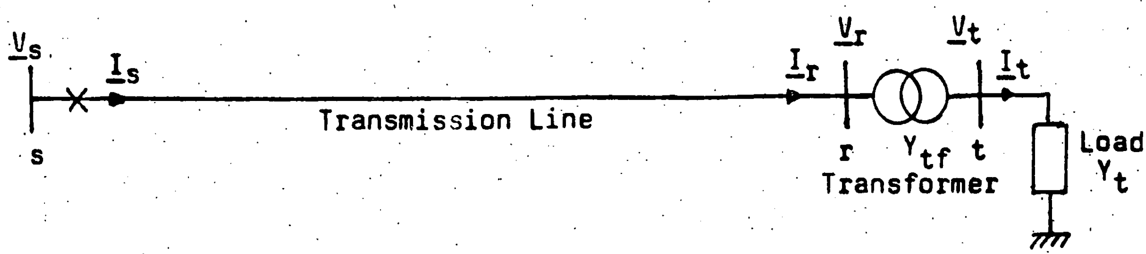


FIG 4 - ENERGISATION OF A LOADED TRANSFORMER

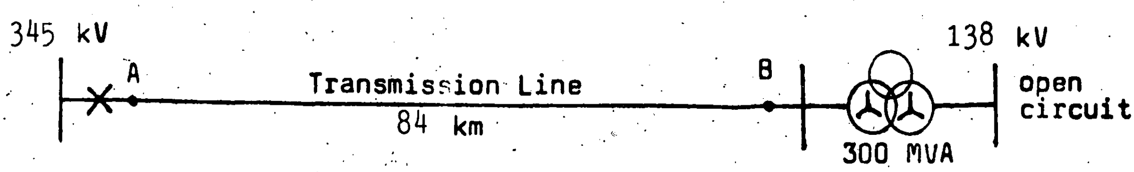


FIG 5 - TRANSFORMER FEEDER SYSTEM USED IN THE ANALYSIS

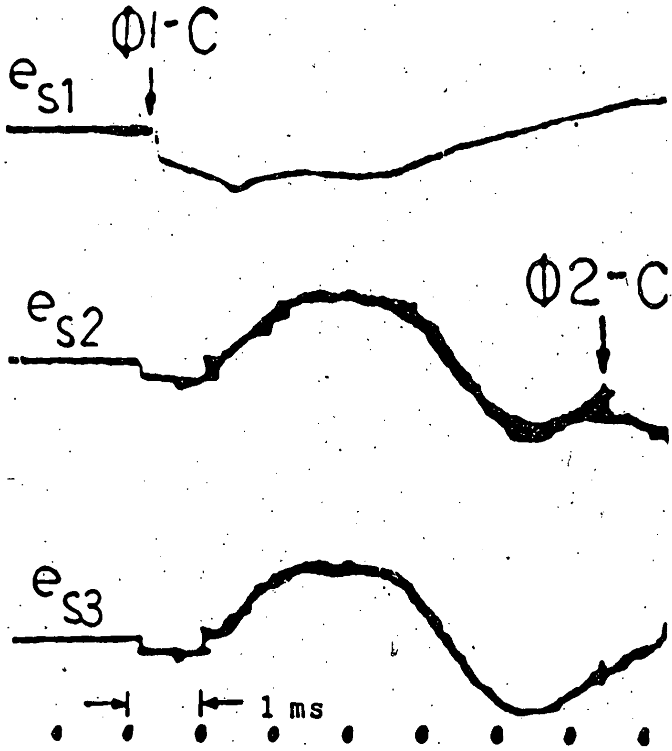


Fig 6(a) Sending end voltage waveforms
(Field Test Results)

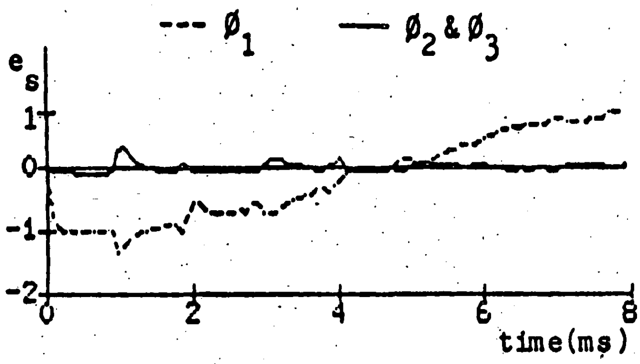


(i) ⅄-⅄-⅄ transformer at r.e.

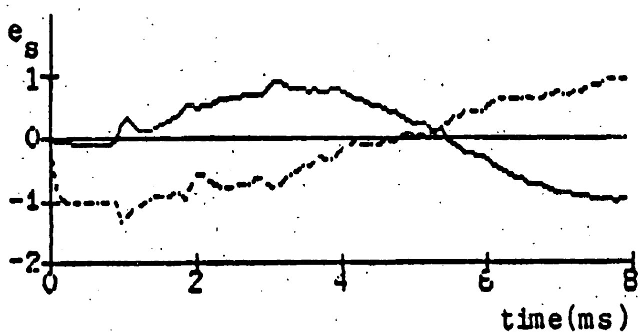


(ii) ⅄-⅄-Δ transformer at r.e.
(without interlimb coupling)

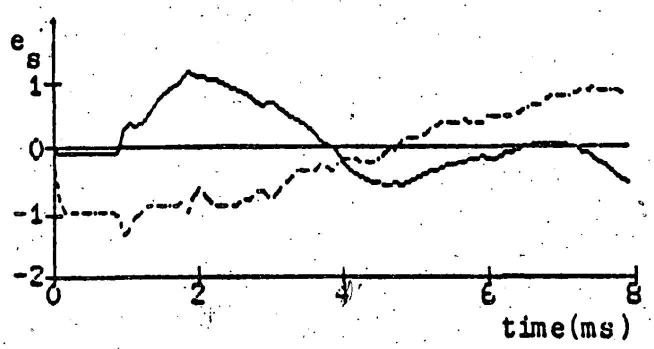


(iii)⅄-⅄-▷ transformer at r.e.
(with interlimb coupling)

Fig 6(b) Sending end voltage waveforms
(Computed Results)

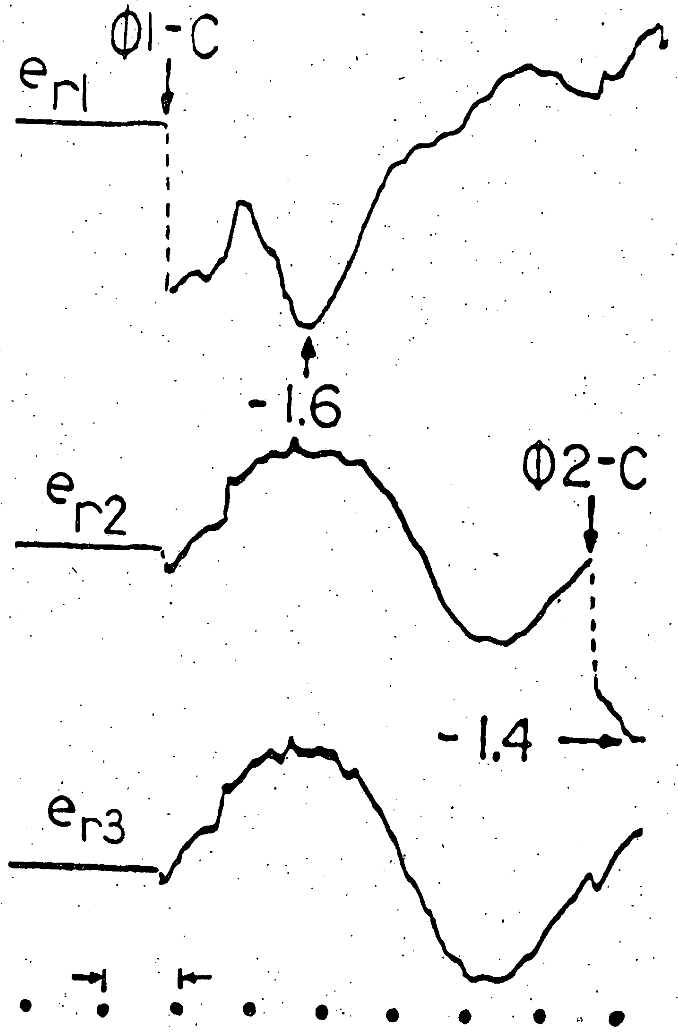


Fig 7(a) Receiving end voltage waveforms
(Field Tests Results)

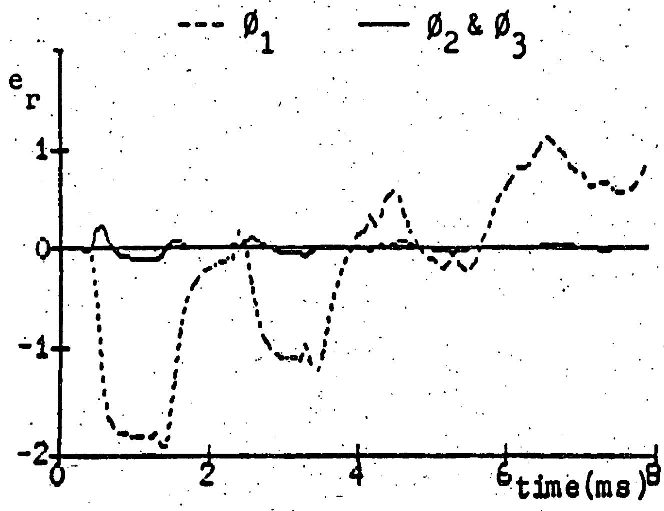


(i) ⅄-⅄-⅄ transformer at r.e.

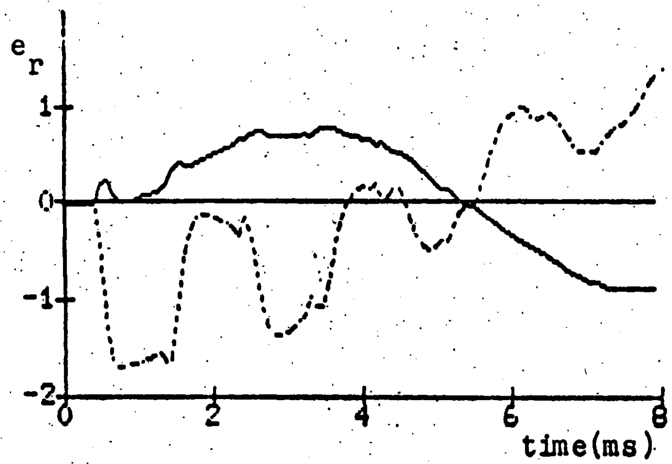


(ii) ⅄-⅄-▷ transformer at r.e.
(without interlimb coupling)

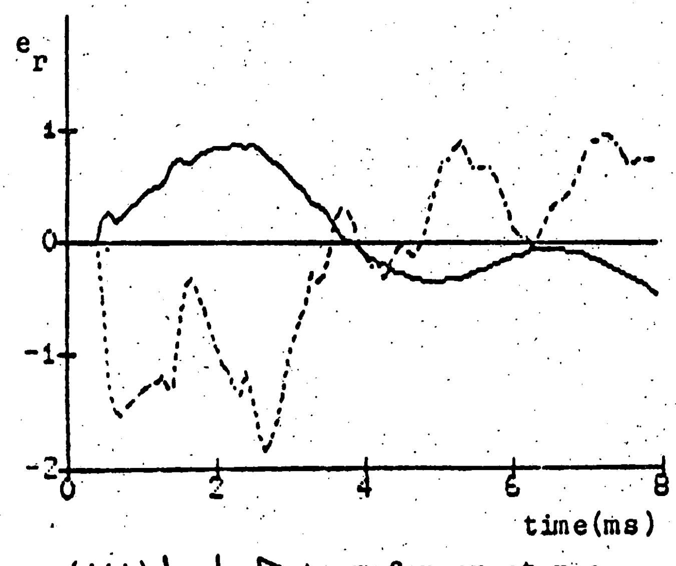


(iii) ⅄-⅄-▷ transformer at r.e.
(with interlimb coupling)

Fig 7(b) Receiving end voltage waveforms
(computed Results)